J. Fluid Mech. (1989), vol. 198, pp. 177–197
Printed in Great Britain

A hydrodynamical theory of conservative bounded density currents

By M. W. MONCRIEFF† AND D. W. K. SO‡

†National Center for Atmospheric Research, Box 3000, Boulder, CO 80307, USA

‡Space and Atmospheric Physics Group, Physics Department, Imperial College, London SW7 2BZ, UK

(Received 15 September 1987 and in revised form 10 June 1988)

The Benjamin (1968) analysis of a two-fluid density current is extended to include the effect of vorticity within the current. In the case of constant vorticity, the density-current depth is shown to lie between the limits of half and two-thirds of the channel depth. More general vorticity distributions are also considered, namely those that have: (i) a maximum in the upper and lower regions of the density current; and (ii) a maximum in the middle of the density current. In the former, as in the case of constant vorticity, density-current structures exist, whereas in the latter, deep overturning circulations predominate which can cause a 'blocking' of the upstream inflow. A generalized propagation formula which includes the effects of finite depth and rear inflow into the density current is established and the uniqueness issue is considered.

The analysis is further extended to a three-fluid system, composed of physically distinct component flows, namely, a density current, an overturning updraught region in upper levels ahead of the density current and an updraught in which the fluid ascends without overturning to its outflow level. Two types of behaviour are identified. First, a symmetric mode in which the density current and the overturning updraught have the same depth and, second, an asymmetric mode with solutions restricted to a certain parameter range. A special case in which the fluids have the same density illustrates the basic dynamics of the problem and also the nature of the vertical transport of momentum.

1. Introduction

This paper examines the dynamics of density currents (or gravity currents, as they are sometimes called) which are constrained to conserve mass, energy and momentum in a vertically bounded domain. It is, however, appreciated that the non-conservation of energy is an important consideration. For instance, in hydraulic jumps or in shallow density currents, momentum and mass can be simultaneously conserved but a loss of total energy to turbulence is essential, a property which results in these systems being fundamentally dissipative. Consequently, mass and momentum conservation are stronger constraints on the dynamics than energy conservation. This aspect was considered at length by Benjamin (1968) who clarified the von Kármán (1940) analysis for the propagation of density currents in an unbounded fluid. It will be shown, however, how the conservative analysis can be extended to non-conservative systems.

A considerable amount of experimental and theoretical work has been performed on density currents in unstratified fluids and generally these studies have been

confined to the propagation of density currents remote from their generation region. The reader is referred to Simpson (1982) for a review in which the ubiquitous nature of density current phenomena is demonstrated. The physical problem is complicated considerably by the inclusion of stratification and localized heating or cooling, because vorticity sources then exist within the fluid. Such complications arise in an atmospheric application of density-current theory and the work reported in this paper is a limiting case of this more complex problem.

The classical two-fluid model of Benjamin (1968) is extended to include vorticity in the density current. In addition, a three-fluid type of density current is developed, the motivation being to understand the basic dynamics of atmospheric squall lines and narrow cold frontal rainbands for which the three-fluid model is an archetype. Only the far-field solutions at large distances from the density-current head are considered. In §2, the classical two-fluid problem is extended, while the three-fluid system is analysed in §3. In order to distinguish between these two types, the terminology of 'two-fluid' and 'three-fluid' density currents will be adopted.

2. Two-fluid models

The flow will be assumed to be steady ($\partial/\partial t = 0$ in a frame of reference moving at the propagation speed of the system), two-dimensional, inviscid, incompressible and not necessarily Boussinesq, so the Euler and mass conservation equations are appropriate,

$$\frac{\mathrm{D}\boldsymbol{v}}{\mathrm{D}t}+\frac{1}{\rho}\nabla p'+g\boldsymbol{k}=0, \tag{2.1}$$

$$\frac{\partial u'}{\partial x}+\frac{\partial w'}{\partial z}=0, \tag{2.2}$$

where $\mathrm{D}/\mathrm{D}t = u'\,\partial/\partial x' + w'\,\partial/\partial z'$. The Bernoulli equation is particularly useful in a steady theory because it represents energy conservation,

$$\tfrac{1}{2}\boldsymbol{v}^2+\frac{p'}{\rho}+gz'=f(\psi), \tag{2.3}$$

where $f(\psi)$ is a streamline variable.

The following classical cases serve to introduce the theoretical problem. In the density-current problem in a channel, considered by Benjamin (1968), stagnant fluid of negligible density intrudes along the horizontal upper boundary into a denser fluid. The depth of the density current is shown to be equal to half the depth of the channel so $h' = \frac{1}{2}H'$, the inflow is subcritical ($U_0' = \frac{1}{2}(gH')^{\frac{1}{2}}$) and the outflow is locally supercritical ($U_1' = (2gh')^{\frac{1}{2}}$). It was also shown that a wavetrain extending downstream cannot exist in conservative flows so the solution is mathematically unique. Furthermore, for a shallow density current (h'/H' small), wave breaking at the density-current head is inevitable so that the flow is locally non-conservative.

The case of a stagnant fluid ($\rho = \rho_b$) intruding along the bottom boundary into a less dense fluid ($\rho = \rho_a$), is mathematically analogous to the above model. Defining $\hat{g}_b = g(\rho_b - \rho_a)/\rho_a$, it can be shown that

$$h' = \tfrac{1}{2}H', \quad U_0 = \tfrac{1}{2}(\hat{g}_b H')^{\frac{1}{2}}, \quad U_1' = (2\hat{g}_b h')^{\frac{1}{2}}.$$

This will be referred to as the Benjamin solution.

The analysis of von Kármán (1940) concerns an infinitely deep overlying fluid. In

this case, the inflow Froude number is expressed as $U_0'/(\hat{g}_b h')^{\frac{1}{2}} = \sqrt{2}$ instead of the $\frac{1}{2}$ that holds for a bounded fluid. Benjamin (1968) argued that energy could not be conserved in shallow, steady and irrotational density currents. This repudiates the von Kármán (1940) results for a density current in an infinitely deep fluid.

2.1. *Density current models containing an internal circulation*

In the Benjamin (1968) model it is assumed that the fluid within the density current is motionless in a frame of reference moving at its propagation velocity and thus the assumption of hydrostatic pressure within the density current is exact. In the following analysis, the effect of vorticity in the density current on its far-field behaviour is included. The pressure in the density current then cannot be exactly hydrostatic except in the far-field where the flow is horizontal.

The physical basis for the problem considered in this paper considerably differs from that associated with 'dam-break' initial conditions in which it is appropriate to assume that the density current has zero vorticity. In atmospheric density currents, however, the physical situation is complicated not only by sources of vorticity generated by the localized heating or cooling of a multiphase state (not considered here) but also by the density-current inflow having non-zero vorticity. Atmospheric density currents frequently originate as outflows of cold air from precipitating convection, within which there is a generation of vorticity arising from horizontal gradients of density. In another atmospheric example, the outflow from an intense descending column of air ('downburst') diverges on encountering the ground and subsequently behaves like a density current; these outflows generate the notoriously dangerous low-level wind-shears which have resulted in a number of aircraft disasters. Since these downbursts are caused by the cooling arising from the evaporation of precipitation, non-zero vorticity is generated within the outflow. In general, the low-level flow towards the head region is an important characteristic of density currents.

Referring to figure 1(*a*), let the surface inflow speed at the rear of the density current be U_s, and the change in pressure across the current at its far-field height (h') be $\Delta p_{h'}'$. In the two-fluid case $\Delta p_{h'}' = p_{\mathrm{LT}}' - p_{\mathrm{RT}}'$. By considering the Bernoulli equation along the lower boundary and the interface between the fluids, it follows that

$$U_0' = -(2\hat{g}_b h' + U_s'^2 \rho_b/\rho_a + 2\Delta p_{h'}'/\rho_a)^{\frac{1}{2}}.$$

Compared to the conventional formula, this relationship involves two additional parameters. It is, however, more accurate for density currents that are not shallow compared with the scale depth of the region they occupy. Since, in general, $\Delta p_{h'}' = -\frac{1}{2}\rho_a(U_1'^2 - U_0'^2) - \text{dissipation}$, where U_1' is the downstream out-flow in fluid A, it follows that $\Delta p_{h'}'$ is negative. (It is appropriate to include dissipation in this particular context because the possibility of an unbounded fluid is not precluded.) However, the effect of the pressure field becomes apparent in bounded currents, due to the presence of an upper boundary. The other additional term ($U_s'^2 \rho_b/\rho_a$) is positive and so there is a partial cancellation, making the classical propagation formula more accurate for a bounded density current than might otherwise be expected.

The above formula leads to a revised relationship for the propagation speed of a two-fluid current in a Boussinesq fluid. In the Boussinesq case, it is valid to set $\rho_b/\rho_a = 1$ in the $U_s'^2 \rho_b/\rho_a$ term. The propagation speed (c) in a motionless environment satisfies $c = -U_0'$ so it follows that the specific kinetic energy of propagation ($\frac{1}{2}c^2$) is equal to the sum of the available potential energy in the density current ($\hat{g}_b h'$), the

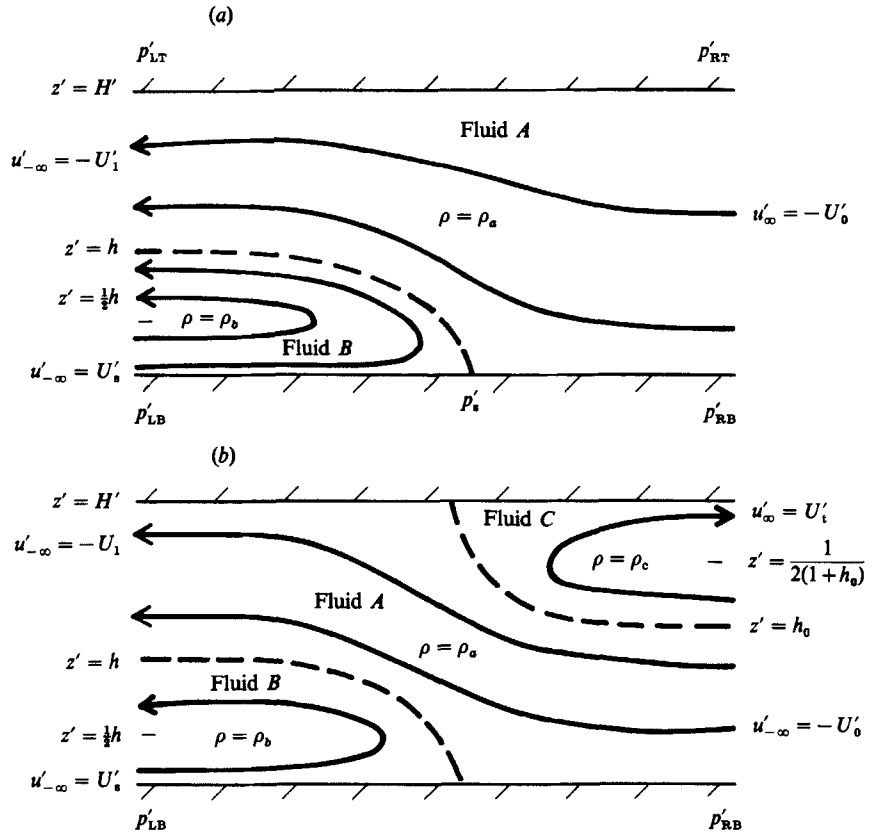

FIGURE 1. Schema of the density current models: (*a*) the two-fluid system consisting of a density current and a jump updraught; (*b*) the three-fluid system having a density current, a jump updraught and an overturning updraught.

maximum specific kinetic energy of the relative inflow ($\frac{1}{2}U'^2_s$) into the density current and the work done by the far-field change in pressure at height h', ($\Delta p'_{h'}/\rho_a$). This is to be compared with the classical formula for an unbounded fluid given by von Kármán (1940) and Benjamin (1968), where $\frac{1}{2}c^2$ is simply equal to the available potential energy.

In a numerical model of density currents in a vertically bounded domain, Crook & Miller (1985) found that if a flow existed within the density current, its propagation speed was in excess of that predicted for an unbounded fluid, namely $c = (2\hat{g}_b h')^{\frac{1}{2}}$. Moreover, it was also shown that as the upper boundary was lowered sufficiently, the propagation speed approximated to the value correspnding to a Froude number of $\sqrt{2}$. These results are consistent with the above theoretical conclusions.

In the present context, the intersection of the density current with the lower boundary is a stagnation point, so it follows from the Bernoulli equation that the propagation speed is simply related to the pressure rise at the stagnation point. It is obvious that

$$c = -U'_0 = (2\Delta p'_s/\rho_a)^{\frac{1}{2}},$$

where on referring to figure 1(*a*), $\Delta p'_s = p'_s - p'_{RB}$. This expression is attractive because it does not directly involve the kinematics of the flow within the current.

There are two distinct branches of flow shown in the two-fluid problem in figure 1(*a*), namely an ascending 'jump' in the less dense fluid (region A) and an 'overturning' in the density current (region B). In the present context, 'jump' refers to the elevated behaviour of the streamlines and should not be confused with a hydraulic jump, which is generally a dissipative phenomenon. These two branches are assumed to be of individually constant density and separated by an interface vortex sheet. In region A, the inflow is horizontal and of constant speed $(-U_0')$ and since the fluid is unstratified, the vorticity is identically zero. In region B, the density current, the far-field flow is again horizontal and the vorticity (η) is a non-zero constant, $\eta = -2U_s'/h'$. The far-field velocity in this region is $u'_{-\infty}(z) = U_s'(h'-2z')/h'$.

A bulk conservation condition can be derived in the usual way by integrating the steady-state horizontal momentum equation, $\operatorname{div}(\rho u' \boldsymbol{v}') + \partial p'/\partial x' = 0$, over a volume of unit width in the transverse (y') direction. The following equation is then obtained by using the divergence theorem and pressure continuity at the interface between the fluids:

$$\int_0^{H'} (\rho u'^2 + p')_{-\infty}\, \mathrm{d}z' = \int_0^{H'} (\rho u'^2 + p')_{\infty}\, \mathrm{d}z', \tag{2.4}$$

where the subscripts $-\infty$ and ∞ denote the far-field variables as $x' \to -\infty$ and ∞ respectively. This condition is frequently, but somewhat ambiguously, called the 'flow force'. Here the more general term 'momentum conservation' will be used with the understanding that the sum of the horizontal momentum flux per unit volume and the pressure is conserved. This is a much stronger constraint than energy conservation.

Define $K_a = (U_1'/U_0')^2, K_b = \rho_b U_s'^2/\rho_a U_0'^2, \lambda_b^2 = \hat{g}_b H'/U_0'^2$, where U_s' is the surface inflow to the density current as $x' \to -\infty$. An inflow Froude number can therefore be defined as $F_b = 1/\lambda_b$. Height, velocity and pressure are non-dimensionalized as $h = h'/H'$, $u = u'/U_0'$, $w = w'/U_0'$ and $p = p'/\rho_a U_0'^2$. The K-parameters can be interpreted as either the normalized momentum fluxes per unit volume or kinetic energies per unit mass. K_a refers to the jump inflow and outflow, while K_b compares the strength of the inflow to the density current and the inflow to the jump. K_b is therefore a relative measure of the intensity of the density-current inflow. It should be noted that F_b is distinct from, but functionally related to, the classical Froude number (F) for a density current because $F_b = Fh^{\frac{1}{2}}$. F^2 is proportional to the ratio of the inflow kinetic energy and the potential energy difference between particles undergoing vertical displacement in the jump region and the density current (the available potential energy) and hence depends on the value of h.

The Froude number used here will be defined as F_b because it represents an *inflow* value which is independent of the depth of the density current. Moreover, the three-fluid problem in the following section will identify an additional Froude number for the overturning updraught (F_c) and it is appropriate to maintain the same vertical scale height (H') in both F_b and F_c. By using (2.4), energy and mass conservation, it can be shown that

$$\tfrac{2}{3}K_b - K_a h + \lambda_b^2 h = 0. \tag{2.5}$$

The case of a stagnant density current is recovered by setting $K_b = 0$ and it can be shown that the resulting equation agrees with (2.4), (2.5) of Benjamin (1968) and the simplified form of (2.6) from Holyer & Huppert (1980). In these cases,

$$K_a(1-h^2) - \lambda_b^2 h(2-h) = 0, \quad 2K_a(1-h) - \lambda_b^2 h(2-h) = 1, \tag{2.6}$$

respectively. The proof of (2.6) requires the identities,

$$\frac{\lambda_b^2 h(2-h)(1-h)}{1+h} = \frac{h(2-h)}{1-h^2} = 1,$$

that hold for the Benjamin model.

Application of the Bernoulli equation to the surface inflow streamlines and to the density-current interface gives the energy conservation relationship

$$K_b = K_a - 2\lambda_b^2 h. \tag{2.7}$$

An equation representing the conservation of mass, momentum and energy is thus obtained by eliminating K_b from (2.5), (2.7) and using the relationship $K_a = 1/(1-h)^2$. Non-zero values of h are given by

$$h = \tfrac{1}{3}[2 - \lambda_b^2 h(1-h)^2]. \tag{2.8}$$

In the special case where the fluids have the same density ($\lambda_b = 0$) it follows that $h = \frac{2}{3}$, but otherwise $h < \frac{2}{3}$. This is an interesting result because for the stagnant density current of Benjamin (1968), $h = \frac{1}{2}$ is the *unique* solution. The additional solutions that arise in the present analysis are due to K_b being a variable. A flow within the density current therefore has a significant effect on its depth and dynamical properties. Furthermore, inspection of the energy equation (2.7) shows that since K_b is non-negative, the local outflow Froude number $F_0 = U_1'(\hat{g}_b h')^{-\frac{1}{2}} \geqslant \sqrt{2}$. Moreover (2.5), together with mass conservation gives, $F_0^2 = 1/(2-3h)$ from which it follows that $h \geqslant \frac{1}{2}$.

Two relationships between K_b, h and the pressure difference acoss the system are readily derived. Let $E_b = (p'_{\mathrm{LB}} - p'_{\mathrm{RB}})/\frac{1}{2}\rho_a U_0'^2$; then applying the Bernoulli equation to the surface streamlines and using the condition that the intersection of the density-current interface with the lower boundary is both a separation and stagnation point,

$$E_b = 1 - K_b. \tag{2.9}$$

Using (2.5), (2.8) and $K_a = 1/(1-h)^2$,

$$K_b = \frac{3(2h-1)}{(1-h)^2}, \tag{2.10}$$

and the subsequent elimination of K_b from (2.9), (2.10) gives

$$E_b = \frac{[h-2(2-\sqrt{3})][h-2(2+\sqrt{3})]}{(1-h)^2}. \tag{2.11}$$

These considerations prove that the solutions $h = \frac{1}{2}$ and $h = \frac{2}{3}$ are each limiting cases of the conservative flow described above. The stagnant density current with $K_b = 0$ corresponds to $h = \frac{1}{2}$ and $F_b = \frac{1}{2}$. If a constant vorticity exists within the density current, then as the density difference between the density current and the jump branches decreases, the absolute value of K_b increases with h to the limit where $h = \frac{2}{3}$ and $K_b^{\frac{1}{2}} = -3$. The range of permissible solutions is therefore $\frac{1}{2} \leqslant h \leqslant \frac{2}{3}$. Unlike the case with a stagnant density current, the solution is not unique but depends on the value of K_b, and more generally on the vorticity within the density current. The surface pressure change across the system is zero when $h = 2(2-\sqrt{3})$, a pressure rise exists if $\frac{1}{2} \leqslant h < 2(2-\sqrt{3})$ and a pressure fall if $2(2-\sqrt{3}) < h \leqslant \frac{2}{3}$. From mass conservation, order-one values of h imply a high outflow speed in the less dense fluid with a surface pressure drop downstream.

Now (2.8) can be expressed as a cubic in h, which represents the simultaneous *conservation of mass, energy and momentum*,

$$\lambda_b^2 h^3 - 2\lambda_b^2 h^2 + (3+\lambda_b^2)\, h - 2 = 0. \tag{2.12}$$

It is easily shown that unless $\lambda_b = O(h = \frac{2}{3})$,

$$h = \frac{2}{3}\left\{1 - \left[\left(\frac{3}{\lambda_b}\right)^2 - 1\right]^{\frac{1}{2}} \sinh\left(\tfrac{1}{3}\sinh^{-1}\left[\left(\frac{3}{\lambda_b}\right)^2 - 1\right]^{-\frac{3}{2}}\right)\right\} \tag{2.13}$$

and this equation has only one physical root.

The solutions for h, occurring in the range $[\frac{1}{2}, \frac{2}{3}]$, correspond to λ_b in the approximate range $[0, 2]$, where the lower bound represents a current with zero density difference, a maximum depth and internal circulation intensity and the upper bound represents the Benjamin solution. The functional dependence of h on λ_b is plotted along with the more general solutions in figure 3 and this also represents a limiting case of the general solutions for the three-fluid system of §3. For a unique solution, the value of K_b must be specified, say by (2.7), which gives another equation relating h and λ_b. The value of K_b varies along the curve on this figure, from $K_b^{\frac{1}{2}} = -3$ when $\lambda_b = 0$ to $K_b = 0$ when $\lambda_b = 2$. Further remarks on the question of uniqueness can be found in §4.

2.2. *Far-field streamline displacements*

An equation for the far-field streamline displacements can be derived from the Bernoulli, mass continuity and hydrostatic pressure equations for the far field. Mass continuity gives

$$\frac{\mathrm{d}z_0}{\mathrm{d}z_1} = U_1. \tag{2.14}$$

If z_0 and z_1 are respectively the inflow and outflow heights of each streamline ψ = constant, the Bernoulli equation for the jump updraught gives

$$U_1^2 = 1 - E_b + 2\lambda_b^2 h. \tag{2.15}$$

Combining (2.14), (2.15),

$$\left(\frac{\mathrm{d}z_0}{\mathrm{d}z_1}\right)^2 = 1 - E_b + 2\lambda_b^2 h. \tag{2.16}$$

Using (2.9) and defining $\alpha^2 = K_b + 2\lambda_b^2 h$, the sum of the surface inflow kinetic energy and the available potential energy of a particle at the upper boundary of the density current. On applying the boundary conditions, $z_0 = 0$ when $z_1 = h$ and $z_0 = 1$ when $z_1 = 1$, it follows that

$$z_0 = \alpha(z_1 - h) \tag{2.17}$$

and $\alpha = 1/(1-h)$. Since $\frac{1}{2} \leqslant h \leqslant \frac{2}{3}$, the value of α satisfies $2 \leqslant \alpha \leqslant 3$. The far-field streamline displacement, $\delta(z_0) = (z_1 - z_0)$, is therefore a linear function of the inflow height z_0,

$$\delta(z_0) = h(1 - z_0). \tag{2.18}$$

The streamline displacements within the density current satisfy $\mathrm{d}z_0/\mathrm{d}z_1 = -1$ and so the inflow and outflow speeds on each streamline must be equal, that is $U_1(z_1) = -U_0(z_0)$. Application of the boundary conditions show that the streamline displacements are $\delta(z_0) = h - 2z_0$.

2.3. *Non-constant vorticity in the density current*

The far-field solutions for a stagnant current and those for a current having constant vorticity have been shown to be significantly different. It is therefore instructive to examine the effect of a non-constant vorticity distribution. General far-field vorticity distributions would not significantly complicate the mathematics because there is no generation of vorticity. However, two particular far-field velocity profiles, $u_{-\infty}(z)$ in the range $0 \leqslant z \leqslant h$ serve as useful examples.

First, the sinusoidal profile,

$$u_{-\infty}(z) = \alpha_1 \sin\gamma\pi\left(\frac{1}{2}-\frac{z}{h}\right), \tag{2.19}$$

where $\alpha_1 = K_b^{\frac{1}{2}} \sin(\frac{1}{2}\gamma\pi)$. With this profile, the far-field vorticity is concentrated in the middle of the density current. The relationship between h and λ_b is given by solutions of the cubic

$$\delta_1 \lambda_b^2 h^3 - 2\delta_1 \lambda_b^2 h^2 + (\delta_1 \lambda_b^2 - 1)\, h + \tfrac{1}{2}(1-\delta_1) = 0, \tag{2.20}$$

where $\delta_1 = 3(1-\sin\gamma\pi/\gamma\pi)/2\sin(\frac{1}{2}\gamma\pi)$ is the ratio of the integrated far-field momentum flux in the density current to that for the constant-shear case. For the special case of $\gamma = 1$, either $h = 1$ or

$$h^2 - h + \frac{1}{\lambda_b^2} = 0. \tag{2.21}$$

Since K_b cannot be negative and by definition $K_a = 1/(1-h)^2$, it follows from (2.7) that h must lie within the range $[\frac{1}{2}, 1]$. The positive root of (2.21),

$$h = \frac{1}{2} + \left(\frac{1}{4} - \frac{1}{\lambda_b^2}\right)^{\frac{1}{2}}, \tag{2.22}$$

is therefore appropriate. Clearly, $\lambda_b \geqslant 2$, with the lower bound representing the conservative Benjamin solution. The solution $h = 1$ is a special case because it represents a total blocking of the jump inflow by an overturning circulation which extends throughout the full depth of the channel. This solution cannot therefore be described as a density current in the conventional sense.

Second, the profile

$$u_{-\infty}(z) = K_b^{\frac{1}{2}}\left(1-\frac{2z}{h}\right) - \alpha_2 \sin\frac{2\pi z}{h}, \tag{2.23}$$

concentrates the vorticity near the top and bottom of the density current. The functional relationship between h and λ_b is given by a cubic of the same form as (2.20), namely

$$\delta_2 \lambda_b^2 h^3 - 2\delta_2 \lambda_b^2 h^2 + (\delta_2 \lambda_b^2 - 1)\, h + \tfrac{1}{2}(1-\delta_2) = 0, \tag{2.24}$$

where $\delta_2 = 1 - 4\beta/3, \beta = 1 + \frac{3}{2}\epsilon^2 - 6\epsilon/\pi$ is the ratio of the integrated momentum flux in the density current to that of the constant-shear case, and $\epsilon = \alpha_2/K_b^{\frac{1}{2}}$, the ratio of the amplitudes of the sinusoidal and constant-shear components of the far-field velocity profile. Clearly, when $\epsilon = 0$ (2.12), and (2.24) are identical. The maximum value of ϵ is $1/\pi$, otherwise outflow would occur for $0 \leqslant z \leqslant \frac{1}{2}$ and hence violate the physical model.

The far-field velocity profiles in the density current are shown in figure 2. It should be noted that, for convenience, the velocity in this figure is normalized by $K_b^{\frac{1}{2}}$, a function of h and λ_b.

The solutions to (2.20), (2.24) can obviously be expressed in analytic form but since these are quite complicated, the depth of the density current as a function of the

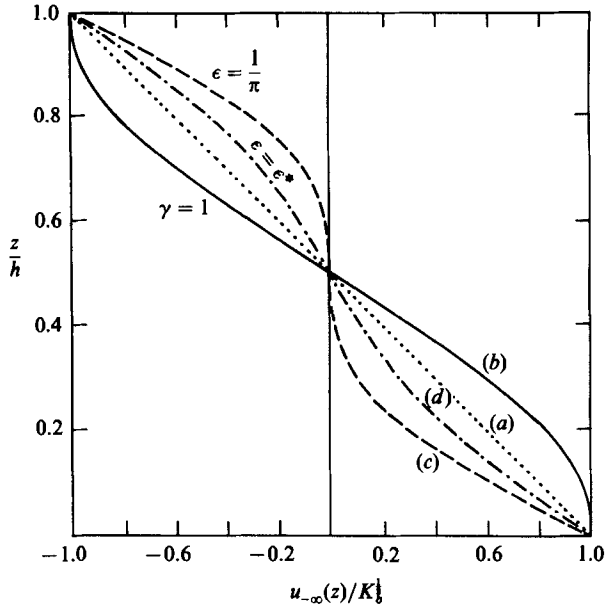

FIGURE 2. The far-field velocity profiles in the density current normalized by K_b. (*a*) ·····, $u_{-\infty}(z)/K_b^{\frac{1}{2}} = 1-(2z/h)$, which also represents the limit of $\epsilon = 0$ in (*c*). (*b*) ——, $u_{-\infty}(z)/K_b^{\frac{1}{2}} = \sin\gamma\pi(\frac{1}{2}-(z/h))/\sin\frac{1}{2}\gamma\pi$ with $\gamma = 1$. (*c*) – – –, $u_{-\infty}(z)/K_b^{\frac{1}{2}} = (1-(2z/h))-\epsilon\sin(2\pi z/h)$ with $\epsilon = 1/\pi$, the upper bound for this profile. (*d*) –·–·–, same as (*c*) except that $\epsilon = \epsilon_*$, the value that gives $h = \frac{1}{2}$ for $0 \leqslant \lambda_b \leqslant 2$. In all these profiles the domain of definition is $0 \leqslant z \leqslant h$.

inverse Froude number for each of the three far-field profiles is shown in figure 3. It should be noted that the value of K_b varies along the curves in this figure, on which the limiting values of $K_b^{\frac{1}{2}}$ are shown.

Evidently, the vorticity distribution within the density current significantly affects the solution and the physical nature of the phenomenon. It is convenient to divide the solutions into three sets, the first two being associated with $\lambda_b < 2$ and the last with $\lambda_b > 2$. Note that $\lambda_b = 2$ represents the Benjamin solution.

The first set is associated with the profile given by (2.23), in which the vorticity is concentrated near the upper and lower boundaries of the density current. The far-field depth of the density current has the constant-vorticity solution as an upper bound for a given value of λ_b, to which it limits as $\epsilon \to 0$. The lower bound is given by the solution with $\epsilon = 1/\pi$. With this type of velocity profile the depth of the density current is depressed below the Benjamin value of $h = \frac{1}{2}$ provided that $\epsilon > \epsilon_*$, where

$$\epsilon_* = \frac{2}{\pi}\left(1-\sqrt{1-\frac{\pi^2}{24}}\right) \approx 0.15$$

is the special case where $h = \frac{1}{2}$ for *all* λ_b in the range $[0, 2]$.

The second set has the constant-shear solution as a lower bound with the upper bound being the full depth of the channel. As γ increases towards unity, the flow from ahead of the current becomes progressively more blocked and an overturning circulation predominates. In the limit, represented by (2.22) with large values of λ_b, the circulation is of the form schematically shown by the left-hand branch of figure 4(*a*) with a stagnant right-hand branch. This is clearly not a density-current type of regime and its physical interpretation is somewhat obscure. It can be

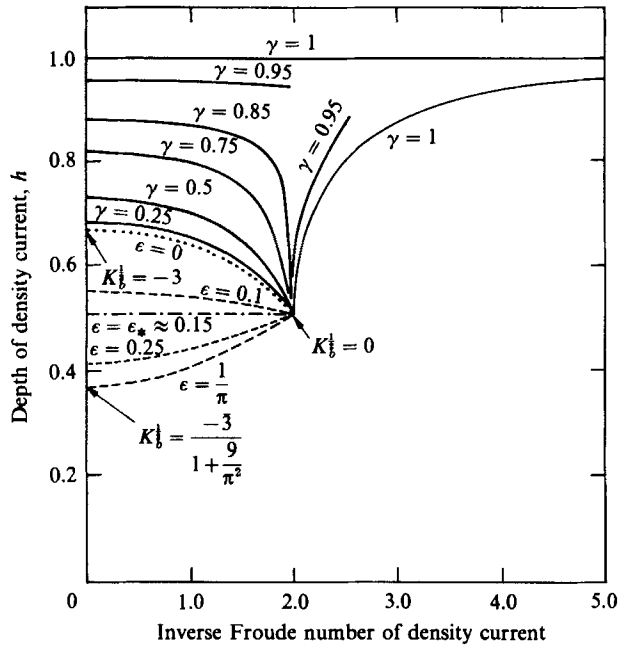

FIGURE 3. The variation of the density-current depth (h) with the inverse Froude number (λ_b) for the far-field velocity profiles shown in figure 2.

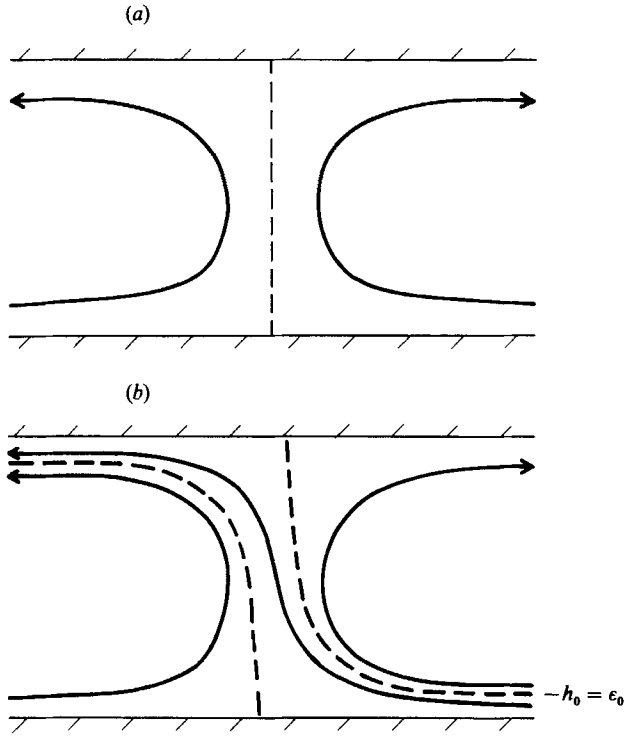

FIGURE 4. Schema of special cases for the uniform-density model: (*a*) pure overturning regime; (*b*) overturning with a jump with an infinitesimal inflow depth.

interpreted, however, as a disturbance moving at a (constant) flow speed within a channel and may represent a form of 'slug' flow (Wallis & Dobson 1973).

The third set associated with velocity profiles given by (2.19) is dominated by a similar type of deep circulation, except in the neighbourhood of $\lambda_b = 2$. The limit as $\lambda_b \to \infty$ also represents the full-depth circulation.

In view of the physical nature of the solutions, it is concluded that density currents are associated with vorticity distributions which are either zero, constant or have a maximum in upper and lower regions, with the stagnant (Benjamin) density current being a special case.

3. Three-fluid models

The model to be considered here is shown in figure 1(*b*), in which the updraught inflow *bifurcates* into the so-called jump and overturning branches. The cases considered in the last section are limits for which the inflow into region A is always constrained to outflow to the rear. However, in certain meteorological examples of density currents and squall lines, a proportion of the relative inflow overturns and flows out in the propagation direction of the density current; a bifurcation of the stream function therefore exists at the interface between regions A and C in figure 1(*b*). This should be contrasted with the pure 'steering level' regime of Moncrieff (1978, 1981), in which *all* the updraught inflow air overturns, which represents another limit.

The three-fluid model consequently involves an interdependence of three component branches. Regions A and B are analogous to those considered in the last section except that the jump inflow is restricted to $0 \leqslant z_0 \leqslant h_0$ while the inflow in the overturning updraught (region C) occupies the layer $h_0 \leqslant z_0 \leqslant \frac{1}{2}(1+h_0)$. For analytic simplicity each branch in the three-fluid model is assumed to have a constant vorticity.

Applying the Bernoulli equation along the upper horizontal boundary and fluid interface, an analogous equation to (2.7) can be defined for the overturning updraught region,

$$K_c = 1-2\lambda_c^2(1-h_0), \tag{3.1}$$

where $K_a = h_0^2/(1-h)^2$, $K_c = \rho_c U_t'^2/\rho_a U_0'^2$, $\lambda_c^2 = \hat{g}_c H'/U_0'^2$, $\hat{g}_c = g(\rho_a-\rho_c)/\rho_a$ and U_t' is the overturning updraught outflow speed at the upper boundary. Using (2.4), (2.7), (3.1) and the hydrostatic pressure equation as $x \to \pm\infty$, an equation representing the *conservation of mass, energy and momentum* for the three-fluid problem is obtained,

$$\left(\frac{2h_0}{3}-\frac{1}{6}\right)-\tfrac{1}{6}\lambda_c^2(1-h_0)^2-K_a\left(\frac{1}{2}-\frac{2h}{3}\right)+\tfrac{1}{6}\lambda_b^2 h^2 = 0. \tag{3.2}$$

This equation is symmetric in h and $1-h_0$, so it is identically satisfied by the symmetric solution, $h = 1-h_0$, for which momentum conservation ceases to be a constraint. Using mass conservation to eliminate K_a and defining

$$f(h) = (3-4h)/(1-h)^2,$$
$$h_0^2[\lambda_c^2+f(h)]-2h_0(2+\lambda_c^2)+(1+\lambda_c^2-\lambda_b^2 h^2) = 0. \tag{3.3}$$

It should be noted that (3.3) is, in effect, an expression for the conventional density-current Froude number ($F = U_0'/(\hat{g}_b h')^{\frac{1}{2}}$) because $1/F = \lambda_b h$. Consequently, F is a function of the three variables h_0, h, and λ_c.

There are two upper bounds on the values λ_b and λ_c imposed by (2.7), (3.1), because K_b and K_c cannot be negative, namely

$$\lambda_b^2 \leqslant \frac{h_0^2}{2h(1-h)^2}, \tag{3.4}$$

$$\lambda_c^2 \leqslant \frac{1}{2(1-h_0)}. \tag{3.5}$$

The condition for real roots of (3.3) is not particularly informative. Since the general solutions to (3.3), (3.4), (3.5) are not easy to interpret, it is useful to consider simplifications. These relate to the solutions derived in previous sections that are limits of the general solutions.

3.1. *Two-fluid limits*

(i) $\lambda_c = 1, h_0 = \frac{1}{2}, h = 0$. In this case the density current is absent so λ_b is physically undefined and can be set to zero. A stagnant overturning updraught exists, representing the Benjamin (1968) model except that the flow direction is reversed. If $h = 0$ but a flow exists in the overturning updraught, so that λ_c and h_0 are allowed to vary, then the solution to (3.3) is $h_0 = (1+\lambda_c^2)/(3+\lambda_c^2)$ and (3.5) is satisfied in the range $\frac{1}{3} \leqslant h_0 \leqslant \frac{1}{2}$. The lower limit represents an overturning updraught having a maximum depth ($1-h = \frac{2}{3}$), while the upper limit represents a stagnant overturning updraught.

(ii) $\lambda_b = 2, h_0 = 1, h = \frac{1}{2}$. This represents a stagnant density current with a full-depth jump inflow ($h_0 = 0$) so that λ_c is physically undefined and can be set to zero. If h_0 remains equal to unity but h and λ_b^2 are allowed to vary, then from (3.3),

$$\lambda_b = \left[\frac{(2-3h}{h}\right]^{\frac{1}{2}} \Big/ (1-h)$$

and (3.4) is satisfied only in the range $\frac{1}{2} \leqslant h \leqslant \frac{2}{3}$. From the solution in §2.2 the upper-bound for λ_b is 2.

(iii) $\lambda_b = 0, h_0 = 1, h = \frac{2}{3}$. This combination of parameters represents a density current having a vanishingly small density difference, an internal circulation of maximum intensity and a maximum depth of $h = \frac{2}{3}$.

(iv) $\lambda_c = 0, h_0 = \frac{1}{3}, h = 0$. This represents an overturning updraught branch having a vanishingly small density difference and a circulation of maximum intensity and depth and no density current. This is the inverted counterpart of (ii).

3.2. *Symmetric solutions*

It is illuminating to consider the simpler symmetric problem in which the overturning updraught and the density current have the same depth, so that $h_0 = 1-h$. In this case let $\lambda_b = \lambda_c = \lambda_*$ and $F_b = F_c = F_*$ (say) in which case $\rho_a = \frac{1}{2}(\rho_b + \rho_c)$. The inequalities given by (3.4), (3.5) require that $\lambda_*^2 \leqslant 1/(2h)$ and hence large values of λ_* (small F_*) are possible only if h is small, that is if both overturning regions are shallow. Note that the flow need not be symmetric unless density is uniform.

In the symmetric case, the conservation equation (3.2) is satisfied identically and the behaviour of the solutions is therefore determined by (2.7), (3.1). These two equations give identical relationships for the kinetic energy per unit volume, $\rho_b U_s^2$

and $\rho_c U_t^2$ and since $U_1 = U_0$, it is sufficient to consider only the case $K_b = K_c = K_*$ (say). It follows that the set of parameters defining the solutions is $\{K_*, \lambda_*\}$ with,

$$K_* = 1 - 2\lambda_*^2 h. \tag{3.6}$$

In the symmetric case, the density current and overturning regions can extend throughout the full depth of the domain ($h \to 1$), provided that $K \to (1-2\lambda_*^2)$ or alternatively $F_* \to [2/(1-K_*)]^{\frac{1}{2}}$. This requires that $K_* \leqslant 1$ or $\lambda_b \leqslant 1/(2h)^{\frac{1}{2}}$. It follows that *full-depth* symmetric solutions can exist only if λ_b and λ_c are both less than $1/\sqrt{2}$, so that the value of F_b (and the conventional Froude number) should be less than $\sqrt{2}$. These full-depth three-fluid solutions are counterparts of the full-depth two-fluid examples of §2.3.

If the density difference $(\rho_b - \rho_a)$ is fixed then λ_* increases and therefore U_0 decreases. Moreover, for a fixed value of λ_*, U_s decreases as h increases and $h = 1/(2\lambda_*^2)$ represents the limiting case of $U_s = 0$, with an analogous results for U_t.

3.3. *Uniform density*

Another useful special case is when the fluids all have the same density (ρ), so that $\lambda_b = \lambda_c = 0$. In this case, (3.3) simplifies considerably and has the two roots, $h_0 = 1-h$ and $h_0 = (1-h)/(3-4h)$, which represent the symmetric and asymmetric solutions, respectively. For $\frac{1}{2} < h_0 < 1$, h_0 is a rapidly varying function of h, while for $0 < h < \frac{1}{2}$, h is a rapidly varying function of h_0. The pressure change across the system (Δp) is independent of height. For the symmetric case it is zero at all levels while for the asymmetric case it is given by $E_b = (1-h)(1-2h)(\frac{3}{4}-h)^{-2}$ and $K_b = 1 - E_b = (3-4h)^{-2}$. Moreover, from (2.7), (3.1) $U_s = -U_1$ and $U_t = 1$ so that the remote flow speed is continuous at the two interfaces and in the symmetric case $U_s = U_t = -U_1 = 1$.

As discussed previously, there is an upper limit of $\frac{2}{3}$ for the density current depth and a lower limit of $\frac{1}{3}$ for the overturning updraught. For the upper limit, $h = \frac{2}{3}$, $U_s = -U_1 = 3$, $\Delta p/\frac{1}{2}\rho U_0^2 = -8$ and no overturning updraught exists ($h_0 = 1$). For the lower limit, $h_0 = \frac{1}{3}$, $U_t = 1 = -3U_1$, $\Delta p/\frac{1}{2}\rho U_0^2 = \frac{8}{9}$ and there is no lower density current ($h = 0$). Symmetric density currents are given by $h_0 = 1-h$, $U_s = -U_1 = 1$ and $\Delta p = 0$.

The uniform-density model is convenient framework to examine the distinction between systems consisting of overturning branches *only* and those having overturning *and* jump branches. In the former, the orientation of the interface between the fluids must be vertical as in figure 4(*a*) and the momentum transport per unit mass must be identically zero at each level. An example of this model is that for $R = 0$ in Moncrieff (1978) with the downdraught flow reversed. If, on the other hand, a jump branch does exist so that the overturning regions do not extend throughout the full depth of the domain, then the system will be tilted away from the vertical with an associated non-zero momentum transport.

Consider the horizontal component of the momentum equation, integrated with respect to x. It follows that since the cross-system pressure difference is constant at each level and $w = 0$ at the lower boundary,

$$\int_{-\infty}^{\infty} (uw)_z \, \mathrm{d}x = \int_0^z (u_{-\infty}^2 - u_{\infty}^2) \, \mathrm{d}z + E_b, \tag{3.7}$$

where $(uw)_z$ denotes the local value of uw at height z and $E_b = 0$ only for the symmetric solution. Since $u_{-\infty}(z)$ and $u_{\infty}(z)$ are known from the far-field solutions, it

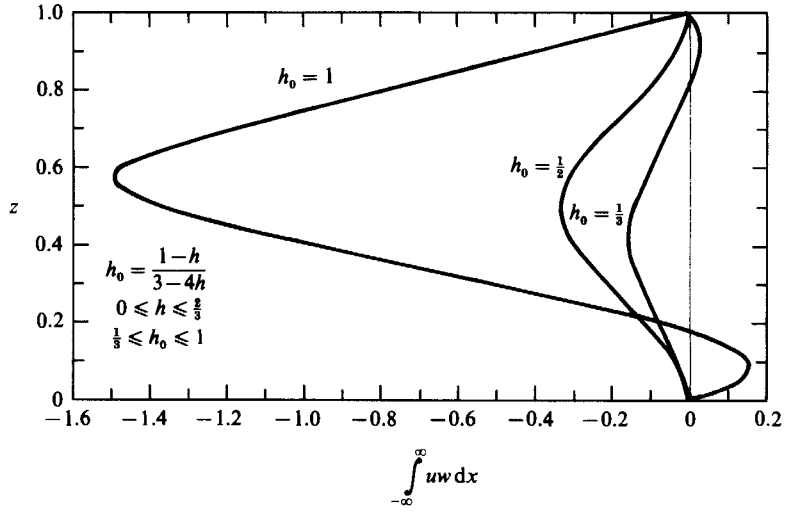

FIGURE 5. The vertical profile of the momentum transport for the constant-density case for selected values of the density-current depth (h) or the jump inflow depth (h_0).

follows that the vertical profile of the momentum transport can be calculated and depends on the value of h_0 (or h) as shown in figure 5. The profile is symmetric for $h = \frac{1}{2}$, while for $\frac{1}{2} < h \leqslant \frac{2}{3}$ and $0 < h \leqslant \frac{1}{2}$, the maximum is displaced above and below $z = \frac{1}{2}$ respectively.

In the asymmetric case it should be noted that since solutions exist only in the range $0 \leqslant h \leqslant \frac{2}{3}$ (corresponding to $\frac{1}{3} \leqslant h_0 \leqslant 1$) this solution is characterized by the presence of both jump and overturning regions. However, in the symmetric case the solution with $h_0 = 0$ is evidently possible, so that the density current and overturning updraught can extend throughout the entire depth of the domain and a jump branch is absent. This solution should limit to the form shown in figure 4(*a*). The limit of $h_0 = 1$ represents the horizontal undisturbed flow with $u = 1$ asymptotically. If $h_0 = \epsilon_0$ (a small number) then the form of the solution is as in figure 4(*b*). In the symmetric case as h_0 increases from zero, the orientation of the system will change from being vertical to progressively more horizontal as $h_0 \to 1$. A rigorous examination of the internal structure and orientation of the system, however, requires the solution of the appropriate internal boundary problem. This generality is, however, beyond the scope of this paper.

Following from the definition of E_b and considering the asymmetric solution, when the density current depth (h) exceeds half the total depth, there is a net pressure drop across the system and the density current is maintained by a faster inflow speed (U_s); the maximum pressure drop exists for $h = \frac{2}{3}$. On the oher hand, when h is less than half the total depth there is a pressure rise and a corresponding decrease in U_s and the maximum pressure rise coincides with $h = 0$. It follows that a shallow density current is associated with high pressure to the rear and a weak inflow, whereas a deep density current coincides with a rearward lowering of the pressure.

3.4. *General solutions*

The general problem in which λ_b and λ_c are unequal is represented by both roots of (3.3) together with the inequalities (3.4), (3.5). Values of λ_b, λ_c and h are specified and the corresponding roots for h_0 calculated. The complicated nature of these solutions

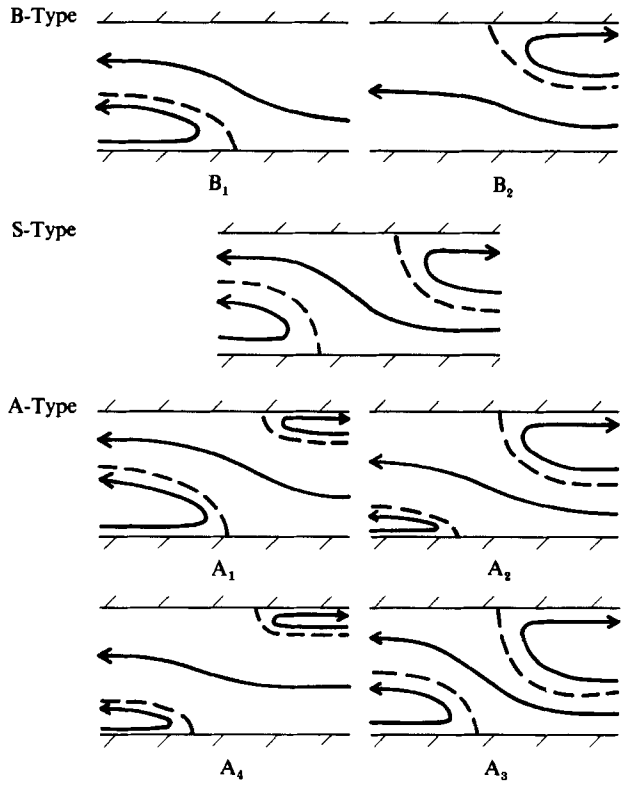

FIGURE 6. Schema of the significant types of flow organization. A description can be found in the text.

is difficult to describe concisely, so a convenient (but probably not unique) classification is used. Consider the three main classes of behaviour schematically shown in figure 6. The two-fluid type B has either a density current or an overturning region and contains the Benjamin solution as a special case. It is appropriate to subclassify B into B_1 and B_2. Type B_1 has a density current with a jump updraught extending throughout the full depth of the domain and coincides with the solution shown in §3.1. Type B_2 has no density current but contains jump and overturning updraughts and includes the case in §3.1. Class S represents the symmetric solutions of §3.2 with $h_0 = 1-h$. The symmetric type can only extend over the full depth of the domain if $\lambda_b \leqslant \sqrt{2}$, as established above in §3.2. Class A represents the asymmetric solutions, and it is useful to consider four different types A_1, A_2, A_3 and A_4. A_1 has a deep density current and a shallow overturning updraught, which degenerates into the B_1 type; A_2 has the converse structure with a shallow density current and a deep overturning updraught, and degenerates into the B_2 type; A_3 has deep density and overturning regions (this is predominantly an 'overturning' regime); A_4 is distinguished by having relative shallow density current and overturning regions. Both A_3 and A_4 are variants of the symmetric S type but they extend over a much wider range of parameter space.

Sets of solutions to (3.3), subjected to the necessary constraints (3.4), (3.5) are shown in figure 7 as contours of h_0 with h and λ_b on the abscissa and ordinate respectively and λ_c a specified parameter. When distinct roots of the quadratic exist these are plotted separately and entitled 'root 1' and 'root 2' on the appropriate diagrams. Evidently, there are significant differences between small and large values

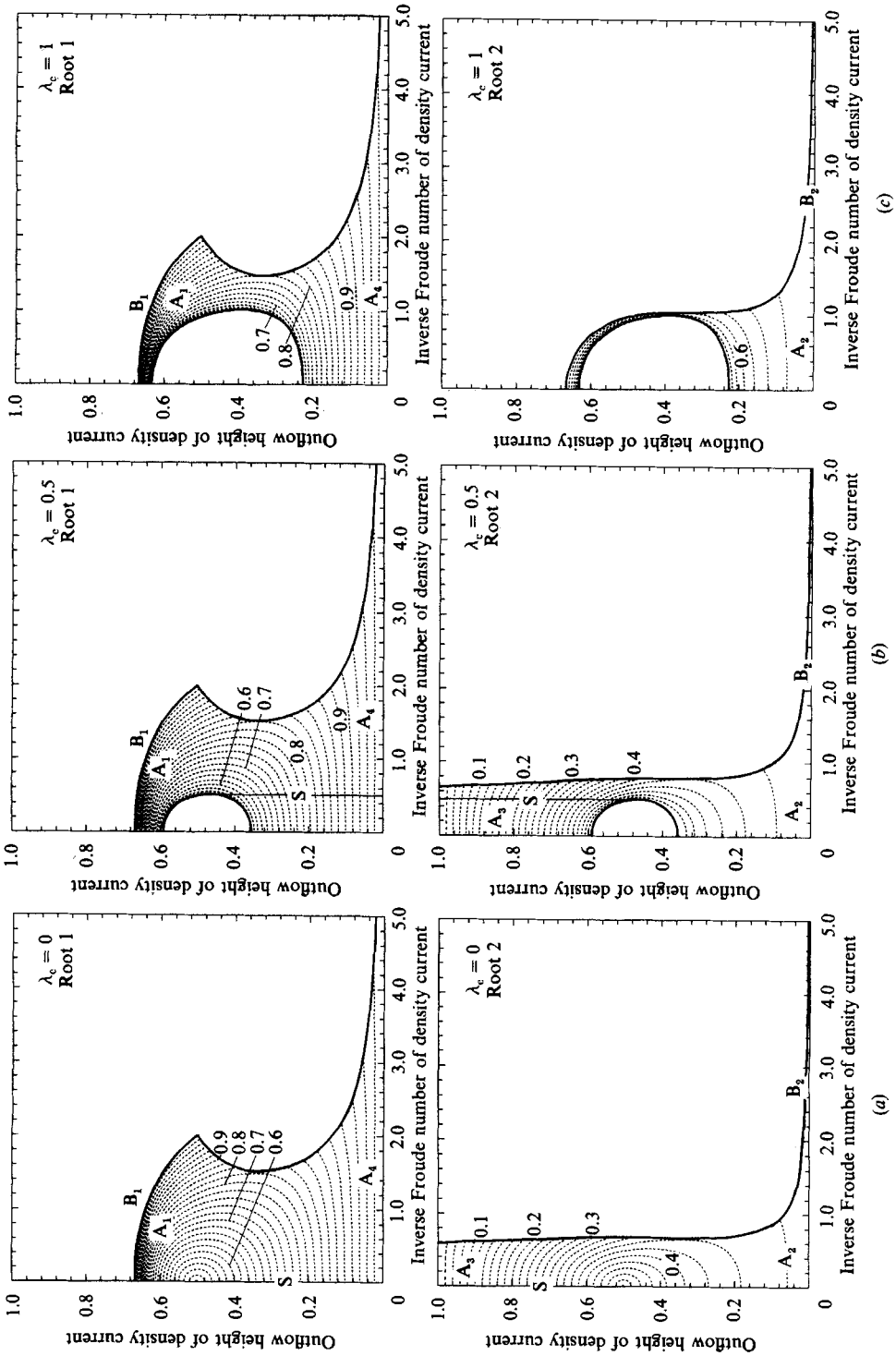
λc = 0
Root 1
λc = 0.5
Root 1
λc = 1
Root 1
λc = 0
Root 2
λc = 0.5
Root 2
λc = 1
Root 2
Outflow height of density current
Inverse Froude number of density current
A1
A2
A3
A4
B1
B2
S
0.1
0.2
0.3
0.4
0.6
0.7
0.8
0.9
(a)
(b)
(c)

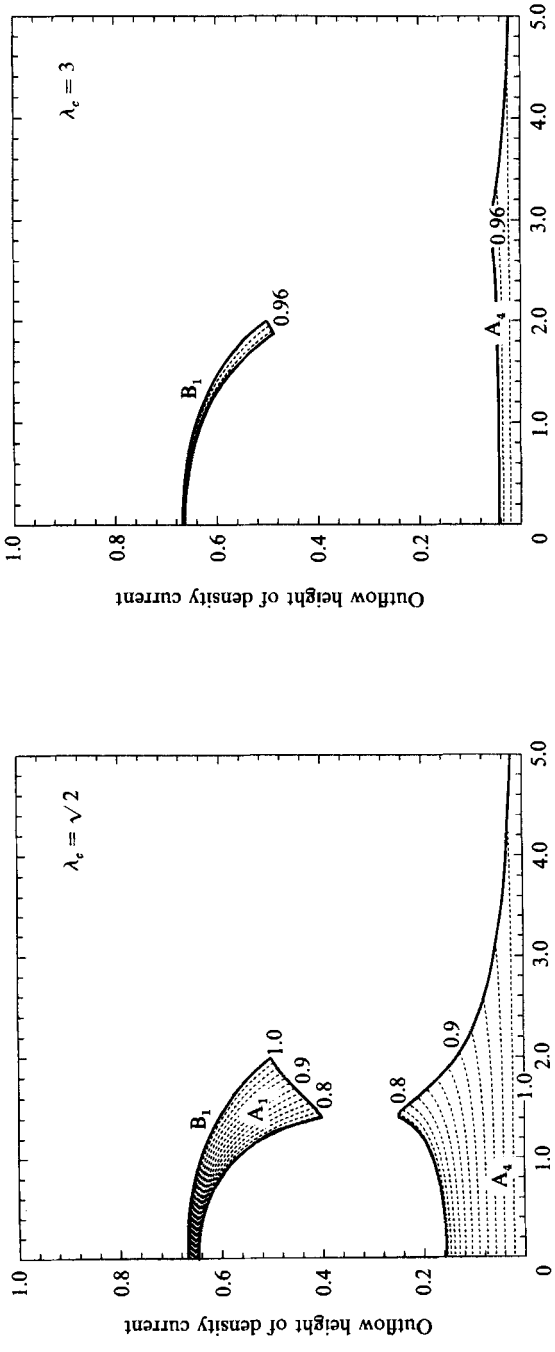

FIGURE 7. Sets of solutions to (3.3), (3.4), (3.5) represented as contours of h_0 with λ_c specified and h and λ_b as variables (*a*) $\lambda_c = 0$; (*b*) $\lambda_c = 0.5$; (*c*) $\lambda_c = 1.0$; (*d*) $\lambda_c = \sqrt{2}$ and (*e*) $\lambda_c = 3.0$. If two real roots exist these are referred to as roots 1 and 2. Only one root exists in cases (*d*) and (*e*). The isoline interval is 0.02.

of λ_c and it is convenient to compare the regimes as λ_c increases from zero towards its maximum value (approximately 4) in which case the solution is given by (3.13) and plotted on figure 3 ($\epsilon = 0$). The general behaviour of the solutions will be discussed by referring to the above classification.

(i) $\lambda_c = 0$, figure 7(*a*). This identifies a special case in which there is a continuous variation of h_0 within the permitted parameter range. The uniform-density models of §3.3 are defined if λ_b is also zero. The symmetric solutions occupy the range $[0, \frac{1}{2}]$ of root 1 and $[\frac{1}{2}, 1]$ of root 2 on the ordinate while the asymmetric solutions occupy the range $[\frac{1}{2}, \frac{2}{3}]$ of root 1 and $[0, \frac{1}{2}]$ of root 2, consistent with the remarks in §3.2. Considering non-zero values of λ_b, the upper part of the root 1 domain represents the B_1 type, which limits to the solution with $\epsilon = 0$ shown in figure 3 for large values of λ_c. The lower portion of the diagram for root 1 defines the A_4 type of structure of shallow density current and overturning updraught branches with a continuous transition to the A_1, B_1 and S types. For root 2, the lower part of the diagram represents the B_2 type. There is a continuous transition to the A_2, A_3 and S types for both roots. For values of λ_b greater than about 2, the root 1 and root 2 solutions asymptote to the undisturbed flow (represented by the abscissa) and the B_2 type (associated with a minimum value of $h_0 = \frac{1}{3}$), respectively.

(ii) $\lambda_c = 0.5$, figure 7(*b*). The above behaviour is maintained for values of λ_c smaller than $1/\sqrt{2}$, with symmetric solutions being possible only if $\lambda_b = \lambda_c$. There is, however, an important distinction between zero and non-zero values of λ_c because in the latter, gaps appear in the solution spectrum. This first becomes evident in the neighbourhood of the point $(\lambda_b = 0, h = \frac{1}{2})$.

(iii) $\lambda_c = 1.0$, figure 7(*c*). An intermediate type of behaviour is illustrated by this case, because for values of λ_b smaller than 1 there is a marked gap in the solution spectrum. First considering root 1, the upper bound for h is again given by the B_1 solution, the typical behaviour of all values of λ_c, while the lower part of this diagram represents an A_4 structure. There is a discontinuous transition to a basically A_1 type behaviour as the density-current depth increases from zero to its maximum value. For $\lambda_b = 1$ there is a continuous transition from A_4 to B_1 passing through A_1 type behaviour. Second, the values of $h_0 = \frac{1}{2}$ for root 2 on the λ_b-axis show that this is the limit to the B_2 solution.

(iv) $\lambda_c = \sqrt{2}$, figure 7(*d*). The discontinuous behaviour of the solutions for intermediate values is well illustrated by this case. Only one root exists, defining either the A_1, A_4 or B_1 types.

(v) $\lambda_c = 3$, figure 7(*e*). Larger values of λ_c represent extreme cases of the A_4 or the B_1 types. It should be noted that the B_1 type is the limit as λ_c increases to its maximum value (≈ 4), and this coincides with the solution $\epsilon = 0$ on figure 3. No overturning updraught exists for values of λ_c in excess of this value, and therefore only two-fluid flow is possible.

The gaps in the spectrum can be explained as follows: (3.5) shows that large λ_c implies a shallow overturning updraught, while the same result follows from (3.4) for the density current when λ_b is large. However, since $h_0 \leqslant 1$, λ_b cannot exceed a critical maximum value. Moreover (3.4), can be written as a cubic relationship in h, namely $h(1-h)^2 \leqslant h_0/2\lambda_b^2$. The cubic $h(1-h)^2 = 0$ attains a maximum of $\frac{4}{27}$ at $h = \frac{1}{3}$ and a minimum at $h = 1$. If $\lambda_b^2 \leqslant \frac{27}{4}h$ then (3.4) is satisfied in the range $0 \leqslant h \leqslant 1$ but if $\lambda_b^2 > \frac{27}{4}$, then (3.4) can be satisfied only within discrete intervals in the neighbourhood of $h = 0$ and $h = 1$. This accounts for the gap between the two ranges of solution and this arises if $\lambda_b^2 > \frac{27}{4} > \frac{27}{4}h_0$. Consequently, shallow overturning updraughts and density currents are associated with 'large' values of λ_b and λ_c.

4. Discussion

The theoretical analysis refers to fluids in which the density differences between the fluids are not necessarily small (non-Boussinesq). This allows the models to be applied to a wide range of multifluid phenomena, including those associated with the channel flow of liquids. Boussinesq theory is a special case and is obtained in the usual way by ignoring the effect of density in the inertial terms but retaining it in the buoyancy terms. Consequently, in the appropriate equations, ρ_b/ρ_a and ρ_c/ρ_a are set to unity, which modifies only the K parameters. The Boussinesq limit is appropriate for density currents and other related phenomena in the atmosphere.

The presence of vortex sheets is a characteristic of the analytic models, and a satisfactory understanding requires the solution of a free-boundary problem for the internal flow, for instance, analogous to that of Moncrieff (1978) for the problems of convection in a stratified shear flow. Moreover, the development of discontinuities from an initial state is important and this aspect should be examined to establish if the steady-state solutions can represent time-asymptotic solutions of the appropriate nonlinear equations. The stability of the vortex sheets is related to the presence of vortices behind the head region and to non-conservation of energy. Such aspects were treated by Benjamin (1968) but although the presence of vorticity in the density current complicates the problem, it is likely that the same general physics applies.

There are physical similarities between the two-fluid solutions of in §2 and those considered by Britter & Simpson (1978) in which fluid was injected with a constant volume flux (Q) into the density current. The form of the flow in the density current in Britter & Simpson (1978) is empirical because the return flow includes mixing with the overlying fluid, and inflow has zero vorticity while the outflow vorticity is non-zero. In the sense that mixing is included in the Britter & Simpson (1978) model and only the mass and momentum equations are solved simultaneously, the approach is essentially non-conservative.

Non-conservative systems can be represented by an approach similar to that in previous sections. For example, in the constant-vorticity model, if the momentum constraint represented by (2.5) and mass continuity are combined but the energy constraint ignored, then (2.12) is replaced by

$$\lambda_b^2 h^3 + (\tfrac{2}{3}K_b - 2\lambda_b^2) h^2 + (\lambda_b^2 - \tfrac{4}{3}K_b - 1) h + \tfrac{2}{3}K_b = 0. \tag{4.1}$$

Solutions can be found by specifying K_b, the counterpart of the non-dimensional volume flux (q) in Britter & Simpson (1978). However, owing to the presence of vorticity within the density current, the solutions will differ from those of Britter & Simpson. An *ad hoc* comparison can nevertheless be made by using the conservative solutions for a specific value of q. Following Britter & Simpson, $q = Q\hat{g}_b/U_0^2$, and if Q is interpreted as the average density-current inflow volume flux then $Q = \frac{1}{2}U_s h$, and

$$q = \tfrac{1}{4}K_b^{\frac{1}{2}} \lambda_b^2 h. \tag{4.2}$$

Using (2.7) and mass continuity it follows that q can be expressed as a function of h only,

$$q(h) = \frac{[3(2h-1)]^{\frac{1}{2}}(2-3h)}{4(1-h)^3}. \tag{4.3}$$

Clearly, q is zero if $h = \frac{1}{2}$ (U_s is then zero) or if $h = \frac{2}{3}$, ($\rho_a = \rho_b$). The maximum value of q is approximately 0.31, corresponding to $h = 0.52$.

The two-fluid theory shows that, in contrast to the Benjamin solution, the depth

of the density current in a conservative flow is not uniquely determined but depends on the value of K_b. In order to close the system it is necessary to make an additional assumption (or formulate an additional constraint) to specify the value of K_b. One of the major conclusions of the extended two-fluid theory is, however, that a wide range of far-field conservative solutions can exist. Holyer & Huppert (1980), in considering energy-conserving flows in the presence of a boundary current, also found non-unique behaviour. The uniqueness criterion used in Holyer & Huppert, in a somewhat different physical problem, was that the volume inflow ($U_0' H'$) should be a maximum because otherwise, it was argued, non-conservative solutions would exist. In the problem considered here H' is fixed, so the Holyer & Huppert condition is equivalent to maximising U_0'. Since the density-current propagation speed increases with its depth, this suggests that the solution with h equal to the maximum value of $\frac{2}{3}$ should be chosen. The same conclusion can be deduced for Boussinesq fluids from a different physical argument. Suppose that the value of K_b is chosen to satisfy continuity of velocity at $z = h$ so that Helmholtz instability, a subsequent breakdown of the density current interface and a transition to turbulence may not be present. Therefore, $U_s = -U_1$ and, since mass continuity gives $K_b^{\frac{2}{3}} = 1/(1-h)$, it follows on using (2.10) that the unique solution is $h = \frac{2}{3}$.

It should be noted that in the three-fluid theory, the overturning updraught region is *not* a density current because horizontal divergence exists in the neighbourhood of the upper stagnation point instead of the convergence that is typical of a density current. The structure of the upper-level flow therefore resembles a wall jet. Significantly, a range of conservative solutions exists in the three-fluid theory but the physical reality of these is considerably more complicated than the two-fluid examples. The distinguishing physical feature of the three-fluid solutions is that either a stagnant region or a circulation exists at upper levels depending on whether K_c is zero or non-zero, respectively. It would be interesting to seek such behaviour in appropriate laboratory experiments, although the technical difficulties in implementing such a study would probably be formidable. For this reason and since the atmospheric applications of density-current theory are of primary interest, it is considered that an evaluation of high-quality field-experiment data or numerical simulations are more promising courses to follow, for instance a rationalization of the structure of squall lines and narrow cold-frontal rainbands by Moncrieff (1988).

In conclusion, a number of additional dynamical effects have been exposed by the inclusion of vorticity within the density current. The physical reality of these steady, conservative solutions is at present under examination and the approach is being extended to include vorticity sources and stratification.

D. W. K. S. acknowledges the support of a Natural Environment Research Council studentship and grant. Comments on the manuscript by A. Crook, B. Foote, M. LeMone, R. Rotunno and anonymous reviewers are acknowledged. The National Center for Atmospheric Research is sponsored by the National Science Foundation.

REFERENCES

Benjamin, T. B. 1968 Gravity currents and related phenomena. *J. Fluid Mech.* **31**, 209–248.

Britter, R. E. & Simpson, J. E. 1978 Experiments on the dynamics of a gravity current head. *J. Fluid Mech.* **88**, 223–240.

Crook, N. A. & Miller, M. J. 1985 A numerical and analytical study of atmospheric undular bores. *Q. J. R. Met. Soc.* **111**, 225–242.

HOLYER, J. Y. & HUPPERT, H. E. 1980 Gravity currents entering a two-layer fluid. *J. Fluid Mech.* **100**, 739–767.

VON KÁRMÁN, T. 1940 The engineer grapples with non-linear problems. *Bull. Am. Math. Soc.* **46**, 615–683.

MONCRIEFF, M. W. 1978 The dynamical structure of two-dimensional steady convection in constant vertical shear. *Q. J. R. Met. Soc.* **104**, 563–567.

MONCRIEFF, M. W. 1981 A theory of organised steady convection and its transport properties. *Q. J. R. Soc.* **107**, 29–50.

MONCRIEFF, M. W. 1988 Analytical models of narrow cold frontal rainbands and related phenomena. *J. Atmos. Sci.* (in press).

SIMPSON, J. E. 1969 A comparison between laboratory and atmospheric density currents. *Q. J. R. Met Soc.* **95**, 758–765.

SIMPSON, J. E. 1982 Gravity currents in the laboratory, atmosphere and ocean. *Ann. Rev. Fluid Mech.* **14**, 213–234.

WALLIS, G. B. & DOBSON, J. E. 1973 The onset of slugging in horizontal stratified air–water flow. *Intl J. Multiphase Flow* **1**, 173–193.